ARTICLE

Quantum Dynamics Study on D+OD$^+$ Reaction: Competition between Exchange and Abstraction Channels

Wen-wu Xu, Pei-yu Zhang*, Guo-zhong He

State key Laboratory of Molecular Reaction Dynamics, Dalian Institute of Chemical Physics, Chinese Academy of Science, Dalian 116023, China

Quantum dynamics for the D+OD$^+$ reaction at the collision energy range of $0.0-1.0$ eV was studied on an accurate *ab initio* potential energy surface. Both of the endothermic abstraction (D+OD$^+\rightarrow$O$^+$+D$_2$) and thermoneutral exchange (D+OD$^+\rightarrow$D+OD$^+$) channels were investigated from the same set of time-dependent quantum wave packets method under centrifugal sudden approximation. The reaction probability dependence with collision energy, the integral cross sections, and the thermal rate constant of the both channels are calculated. It is found that there is a convex structure in the reaction path of the exchange reaction. The calculated time evolution of the wave packet distribution at $J=0$ clearly indicates that the convex structure significantly influences the dynamics of the exchange and abstraction channels of title reaction.

Key words: Time-dependent quantum wave packet method, Potential energy surface, D+OD$^+$ reaction

I. INTRODUCTION

Extensive experimental and theoretical studies have been carried out in order to elucidate the dynamics of O$^+$+H$_2$ reaction and its isotopic variants [1−11]. On the experimental side, Burley *et al.* measured the kinetic energy-dependent rate constant, cross sections and branching ratios of O$^+$+H$_2$ reaction and its isotopic variants D$_2$ and HD using guided ion beam mass spectrometry [1]. Theoretically, Martínez *et al.* developed an accurate analytical ground potential energy surface (PES) of O$^+$+H$_2$ system [3]. Then a serial of calculations [4−7] were performed based on this surface to investigate the dynamics of the O$^+$+H$_2$ reaction and its isotopic variants D$_2$ and HD. However, the H+OH$^+$ reaction, which is the reverse reaction of O$^+$+H$_2$, has been rarely studied. The collision between D and OD$^+$ may lead to two product channels, namely the exchange channel,

$$D + OD^+ \rightarrow D + OD^+ \qquad (1)$$

and the abstraction channel,

$$D + OD^+ \rightarrow O^+ + D_2 \qquad (2)$$

Figure 1 shows the potential energy contour of the minimum energy which is obtained by scanning the

———

*Author to whom correspondence should be addressed. E-mail: pyzhang@dicp.ac.cn
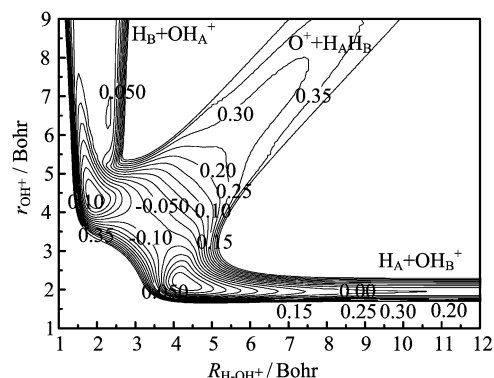
FIG. 1 Potential energy contour diagram of H+OH$^+$ reaction. Energies (in eV) are relative to H+OH$^+$ asymptote.

PES. It is observed that, after entering into the first potential well, the reactants have two channels to leave the well. The first channel is that the reactants directly generate the product of O$^+$+H$_2$ via a steep slope, namely the abstraction channel. Concerning the exchange channel, the reactants must pass over a convex structure to enter into the second potential well. Then they leave the well to generate the product of H+OH$^+$. According to Fig.1 we plot the schematic PES of the both channels in Fig.2, showing the potential energy of the key points (the zero of energy is taken to be the H+OH$^+$ asymptote).

In this work, the time-dependent quantum wave packet method [12−17] under centrifugal sudden (CS) approximation is used to investigate the dynamics of
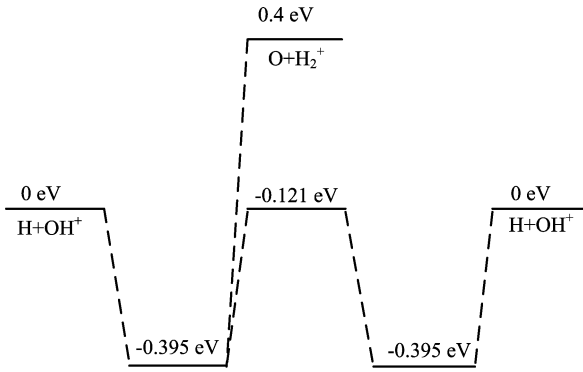
　　　　　　73

FIG. 2 The schematic potential energy surface of the exchange and abstraction channels in the H+OH$^+$ reaction. Energies are relative to H+OH$^+$ asymptote.

the D+OD$^+$ reaction. Usually, the theoretical studies on the ion-molecular reactions have serious difficulties to be performed, since electronically nonadiabatic processes involving different PESs may easily occur [18], due to the energetic proximity of the PES. However, the O$^+$+H$_2$ reaction mainly occurs via the lowest energy quadruplet PES. Therefore, the ground state PES is used to perform the dynamics of the D+OD$^+$ reaction.

II. TIME-DEPENDENT WAVE-PACKET METHOD

In the reactant Jacobi coordinates, the Hamiltonian of the studied system can be expressed as [19, 20],

$$H = -\frac{\hbar^2}{2\mu_R}\frac{\partial^2}{\partial R^2} + \frac{(\hat{J}-\hat{j})^2}{2\mu_R R^2} + \frac{\hat{j}^2}{2\mu_r r^2} + V(\hat{R},\hat{r}) + h(r) \quad (3)$$

where R is the distance from the D atom to the center-of-mass of OD$^+$, r is the OD$^+$ bond length, μ_R is the reduced mass of D with respect to OD$^+$, μ_r is the reduced mass of OD$^+$, J is the total angular momentum, j is the rotational angular momentum number of OD$^+$, and $V(\hat{R},\hat{r})$ is the interaction potential excluding the diatomic potential of OD$^+$, and $h(r)$ is the diatomic reference Hamiltonian. The initial wave packet is expanded in terms of the body-fixed (BF) translational-vibrational-rotational basis $u_n^v(R)\phi_v(r)Y_{jK}^{JM\varepsilon}(\hat{R},\hat{r})$, where n and v are the indices labeling the translational and vibrational eigenfunctions, respectively. ε is the parity of the system. Accordingly, the element of the centrifugal term in the CS approximation is expressed as

$$\frac{\hbar^2}{2\mu_R R^2}\left\langle Y_{jK}^{JM\varepsilon}\right| (\hat{J}-\hat{j})^2 \left|Y_{j'K'}^{JM\varepsilon}\right\rangle =$$
$$\frac{\hbar^2}{2\mu_R R^2}\delta_{jj'}[J(J+1)+j(j+1)-2K^2]\delta_{KK'} \quad (4)$$

where M and K are the projection quantum numbers of J on the space-fixed and BF z-axis, respectively.

TABLE I Parameters for the quantum calculations of the D+OD$^+$ reaction (all quantities are given in a.u., unless otherwise indicated).

Description	Vaule
Centre of initial wave packet on scattering coordinate	14.0
Width parameter of wave packet	0.25
Average translation energy/eV	0.4
Scattering coordinate (R) range	0.1-24
Number of translational basis functions	320
Number of vibrational basis functions	150
$j_{\max}$ for the rotational basis functions	130
Internal coordinate (r) range	0.5-18
Propagation time	90000
Time step	10

Time-dependent Schrödinger equation ($i\hbar\frac{\partial\psi}{\partial t}=\hat{H}\psi$) is solved using the reactant Jacobi coordinates by the split-operator. The total reaction probability, the individual and total reaction cross sections and the rate constant can be calculated by

$$P_{v_0 j_0 k_0}^J(E) = \frac{\hbar}{\mu_r}\text{Im}\left\langle \psi_j(E)\left|\delta(s-s_0)\frac{\partial}{\partial s}\right|\psi_j(E)\right\rangle \quad (5)$$

$$\sigma_{v_0 j_0 k_0}(E) = \frac{\pi}{k^2}\sum_J (2J+1)P_{v_0 j_0 k_0}^J(E) \quad (6)$$

$$\sigma_{v_0 j_0}(E) = \frac{1}{2j_0+1}\sum_{k_0}\sigma_{v_0 j_0 k_0}(E) \quad (7)$$

$$k(T) = \sqrt{\frac{k_B T}{\pi\mu_R}}\frac{1}{(k_B T)^2}\cdot$$
$$\int_0^\infty E\sigma(E)\exp\left(-\frac{E}{k_B T}\right)\mathrm{d}E \quad (8)$$

where $\psi(E)$ is the corresponding time-independent part of the final wave function, k is the wave number corresponding to the initial state at a fixed collision energy E, and k_B is the Boltzmann constant.

III. RESULTS AND DISCUSSION

Table I shows the details of the initial wave packet and other parameters used in the quantum calculations. To obtain the converged results in wave function expansion, 320 sinusoidal translational basis functions are used for the R coordinate within the range of 0.1−24.0 a_0, 150 vibrational basis functions for the r coordinate of 0.5−18.0 a_0, and $j_{\max}$=130 for the rotational basis functions. A propagation time of 9×10^4 a.u. is used for the wave packet initially on the lowest $1^1A'$ state. The width and average translation energy of initial wave packet are 0.25 a_0 and 0.4 eV, respectively.
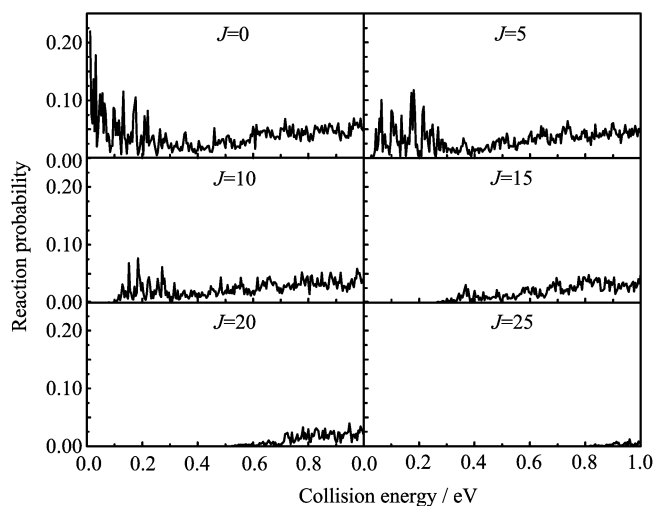
FIG. 3 Reaction probability dependence with collision energy of the exchange channel in the D+OD$^+$ (v_i=0, j_i=0) reaction at total angular momentum J=0, 5, 10, 15, 20, and 25.
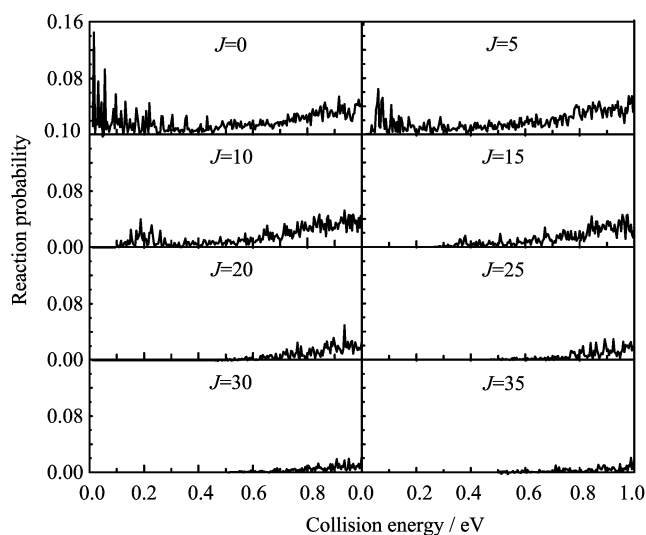

FIG. 4 Reaction probability dependence with collision energy of the abstraction channel in the D+OD$^+$ (v_i=0, j_i=0) reaction at total angular momentum J=0, 5, 10, 15, 20, 25, 30, and 35.

The reaction probabilities of the exchange and abstraction channels in the D+OD$^+$(v_i=0, j_i=0) reaction at different J values are presented in Fig.3 and Fig.4, respectively. As can be seen, the behaviors of the probabilities at different J values for both channels are very similar. The main features of the probabilities for both channels at J=0 are there's dense oscillatory structure with a significant number of high intensity peaks in the low energy range. At higher energies, the peaks are of lower intensity. With the increased J, the density of oscillatory structure gradually becomes smaller. This oscillatory behavior can be attributed to the potential
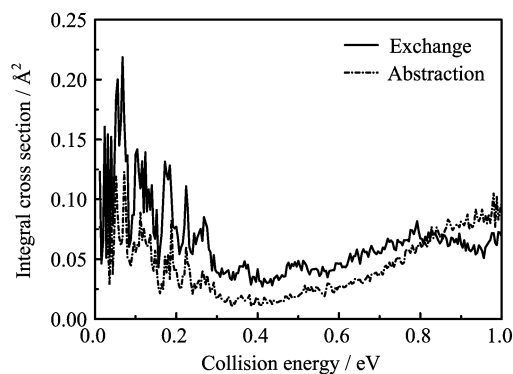

FIG. 5 The integral reaction cross sections of the exchange and abstraction channels in the D+OD$^+$(v_i=0, j_i=0) reaction.
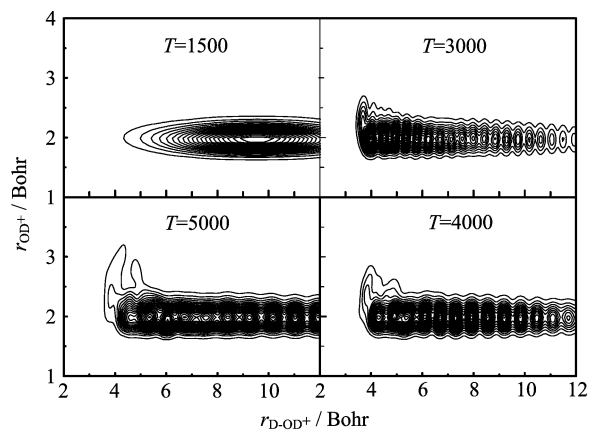

FIG. 6 The time evolution of wave packet distribution of the D+OD$^+$ (v_i=0, j_i=0) reaction at J=0. The horizontal and vertical axes denote R (the distance of D−OD$^+$) and r (the bond length of OD$^+$), respectively.

wells of H+OH$^+$ system. It is also clear that the shifting of the reaction threshold for large J is entirely due to the centrifugal barrier for the intrinsically barrierless reaction. We can also find that the probabilities for exchange channel are larger than that for the abstraction channel at low collision energy while lower at high collision energy.

Figure 5 shows the integral reaction cross sections of the exchange and abstraction channels in the D+OD$^+$(v_i=0, j_i=0) reaction. The wave packet (WP) propagation is performed for J=0−35 in calculations. We find the integral reaction cross sections for both channels show no threshold and are very large at low collision energies, and they will decrease with the increased collision energy. Finally the cross sections reach a plateau for exchange channel, while for abstraction channel, the cross sections continue increasing with the increased collision energy. We find that the cross sections for exchange channel are larger than those for the abstraction channel at collision energy E<0.8 eV and lower at E>0.8 eV. In addition, strong oscillatory struc-
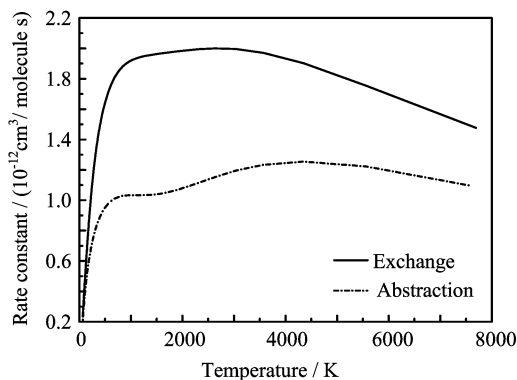
FIG. 7 The thermal rate constant of the exchange and abstraction channels in the D+OD$^+$(v_i=0, j_i=0) reaction.

tures of the cross sections for both channels are also observed.

From Fig.5, we find that the integral reaction cross sections of D+OD$^+$(v_i=0, j_i=0) reaction for both channels are very low. In order to explain this phenomenon, we print the time evolution of WP distribution at J=0 in Fig.6. At propagation time T=1500 a.u., we can see that the distribution gradually enters into the first potential well. While at T=3000 a.u., a rather small part of WP can pass over the convex structure, and the rest is blocked by the convex structure. At propagation time T=4000, and 5000 a.u., the blocked WP is rebounded by the convex structure. In a word, we can conclude from Fig.6 that a great number of WP is rebounded by the convex structure after entering into the first potential well, which results in the low integral reaction cross sections of D+OD$^+$(v_i=0, j_i=0) reaction for both channels. Therefore, the convex structure plays a significant role in the dynamics of the both channels in the D+OD$^+$ reaction.

Finally, we present the temperature dependent rate constants of the D+OD$^+$(v_i=0, j_i=0) reaction in Fig.7. It can be seen that the rate constant for both channels increases with increasing temperature and then decreases at higher temperature. The increase of the reaction rate at lower temperature is much rapid. The rates of exchange channel are much larger than rates of abstraction channel at a given temperature, analogous to the cross section results of Fig.5.

IV. CONCLUSION

In this work, a time-dependent quantum wave packet method under CS approximation was used to investigate the dynamics of the exchange and abstraction channels in the D+OD$^+$(v_i=0, j_i=0) reaction.

The reaction probability dependence with collision energy, the integral cross sections, and the thermal rate constant of the both channels were calculated. The calculated time evolution of wave packet distribution at J=0 clearly indicates that a majority of wave packet cannot pass over the convex structure, leading to much less values of the cross sections in the D+OD$^+$ reaction.

V. ACKNOWLEDGMENT

[1] J. D. Burley, K. M. Ervin, and P. B. Armentrout, Int. J. Mass Spectrom. Ion Process **80**, 153 (1987).
[2] M. González, M. Gilibert, A. Aguilar, and R. Sayós, J. Chem. Phys. **98**, 2927 (1993).
[3] R. Martínez, J. Millán, and M. González, J. Chem. Phys. **120**, 4705 (2004).
[4] R. Martínez, J. D. Sierra, and M. González, J. Chem. Phys. **123**, 174312 (2005).
[5] R. Martínez, J. M. Lucas, X. Giménez, A. Aguilar, and M. González, J. Chem. Phys. **124**, 144301 (2006).
[6] R. Martínez, J. D. Sierra, S. K. Gray, and M. González, J. Chem. Phys. **125**, 164305 (2006).
[7] W. W. Xu, W. L. Li, S. J. Lv, H. S. Zhai, Z. X. Duan, and P. Y. Zhang, J. Phys. Chem. A **116**, 10882 (2012).
[8] M. González, A. Aguilar, and M. Gilibert, Chem. Phys. **131**, 335 (1989).
[9] M. González, A. Aguilar, and M. Gilibert, Chem. Phys. **131**, 347 (1989).
[10] M. González, M. Gilibert, A. Aguilar, and R. Sayós, Chem. Phys. Lett. **204**, 578 (1993).
[11] C. Y. Ng, J. Phys. Chem. A **106**, 5953 (2002).
[12] T. S. Chu and K. L. Han, Annu. Rep. Prog. Chem. Sect. C **108**, 10 (2012).
[13] T. S. Chu and K. L. Han, Phys. Chem. Chem. Phys. **10**, 2431 (2008).
[14] T. S. Chu, Y. Zhang, and K. L. Han, Int. Rev. Phys. Chem. **25**, 201 (2006).
[15] Y. Zhang, T. X. Xie, K. L. Han, and J. Z. H. Zhang, J. Chem. Phys. **119**, 12921 (2003).
[16] T. X. Xie, Y. Zhang, M. Y. Zhao, and K. L. Han, Phys. Chem. Chem. Phys. **5**, 2034 (2003).
[17] T. S. Chu, K. L. Han, and G. C. Schatz, J. Phys. Chem. A **111**, 8286 (2007).
[18] T. S. Chu and K. L. Han, J. Phys. Chem. A **109**, 2050 (2005).
[19] J. Z. H. Zhang, *Theory and Application of Quantum Molecular Dynamics*, Singapore: World Scientific, (1999).
[20] J. Z. H. Zhang, J. Q. Dai, and W. Zhu, J. Phys. Chem. A **101**, 2746 (1997).